Quantum and classical mobility determination of the dominant scattering mechanism in the two-dimensional electron gas of an AlGaAs/GaAs heterojunction

J. P. Harrang, R. J. Higgins, and R. K. Goodall
Department of Physics, University of Oregon, Eugene, Oregon 97403

P. R. Jay, M. Laviron, and P. Delescluse
Thomson-CSF, Laboratoire Central de Recherches, Domaine de Corbeville, B.P. 10 91401 Orsay, France
(Received 7 August 1984)

Recent theoretical and experimental interest has focused on the issue of the dominant scattering mechanism which limits the mobility of the two-dimensional electron gas formed at the molecular-beam-epitaxy (MBE) interface of an AlGaAs/GaAs heterojunction. Measurements have been made at 1.3 K with MBE-grown AlGaAs/GaAs heterojunctions, indicating a difference of nearly an order of magnitude between transport scattering times, expressed as a mobility, measured via either the Hall mobility (classical scattering time) or from the de Haas—Shubnikov oscillation envelope (quantum scattering time). This result is contrasted with measurements from the qualitatively different Si metal-oxide-semiconductor field-effect transistor (MOSFET) interface where, over the same charge-density region, the two mobilities are nearly equal and limited by interface roughness scattering. The ratio of the quantum-to-classical scattering time from competing scattering mechanisms is calculated. The observed low ratio in the heterostructures is in excellent agreement with the calculated screened-Coulomb scattering from residual charge centers in the AlGaAs, while the lack of this effect in the MOSFET's is in excellent agreement with the surface roughness calculation. The measured scattering-time ratio is thus a new method of directly selecting the dominant scattering mechanism among competing effects. Stray effects which could interfere with the quantum measurements are discussed.

I. INTRODUCTION

Molecular-beam-epitaxy (MBE), modulation-doped heterojunctions with very high ($>10^6$ cm^2/V s) mobilities have led to both fundamentally (quantum Hall effect) and technologically (high-speed circuits) significant discoveries. There is a need to understand the scattering in the two-dimensional electron gas (TEG) which forms at the AlGaAs/GaAs heterojunction interface. Field-effect transistor devices made from MBE heterojunction layers have several popular acronyms; we will use TEGFET for two-dimensional electron-gas field-effect transistor. The devices studied were gated so that the TEG density N could be varied from its maximum value at zero gate bias down to $N=0$ (pinch-off). A preliminary report was presented earlier.[1]

Figure 1 shows the conduction band and device layout for a TEGFET. Measured mobilities[2] of TEGFET's can be in excess of 2×10^6 cm^2/V s at 5 K due to the spatial separation of the ionized Si donors by an undoped buffer layer and the lattice matching of the AlGaAs/GaAs interface. Because the heterojunction interface can be nearly perfect, the dominant low-temperature scattering mechanism in the TEG layer is of current theoretical[3,4] and practical interest.

This paper presents measurements of the transport scattering time and a technique of analyzing the results which indicates that the dominant scattering contribution is from ionized impurities in the AlGaAs layer. Scattering contributions from ionized impurities, interface roughness, and alloy disorder are considered. Measurements made on the same TEGFET sample are presented from both classical bulk transport characterization, and Shubnikov—de Haas (SdH), measurements which isolates the TEG. The test pattern includes, within a 0.6-mm^2 re-

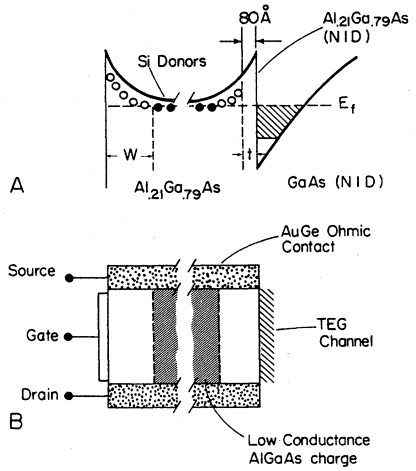

FIG. 1. (A) The conduction-band diagram for a MBE AlGaAs/GaAs modulation-doped heterojunction. (B) The heterojunction TEGFET consists of a Schottky gate and Au-Ge alloy Ohmic source and drain contacts connected to the TEG. Upon applying a negative gate bias, the gate Schottky depletion width increases, first depleting the AlGaAs charge, and then decreasing the TEG density.

gion of MBE material, six short-gate TEGFET's [for geometric magnetoresistance (GMR) and SdH with varying length-width ratios] and a gated van der Pauw pattern for Hall measurements. The 1-μm GaAs MBE layer was grown on a semi-insulating GaAs substrate with a 80-Å undoped AlGaAs buffer and a top $Al_{0.21}Ga_{0.79}As$ layer of 1200 Å (doped with Si to 6×10^{17} cm^3) with a recessed gate. Results from two MBE heterojunction wafers are presented in this paper. The Hall mobility of the "high-mobility" wafer was 117000 cm^2/V s at 1.3 K. The second "low-mobility" wafer had a 1.3-K Hall mobility of 40000 cm^2/V s.

Extensive study, both experimental[5] and theoretical,[6,7] has been done on scattering mechanisms in the TEG that forms at the SiO_2/Si interface of metal-oxide-semiconductor field-effect transistors (MOSFET's). In contrast to the AlGaAs/GaAs heterojunction, the SiO_2/Si interface is rough on an atomic scale and this roughness limits the TEG mobility except at very low electron densities, where Coulomb scattering is dominant.[8] Earlier studies[5] have indicated that in Si the scattering times measured by classical techniques, geometric magnetoresistance (GMR), and quantum methods, SdH, are equal. Since surface-roughness scattering is one of the possible scattering mechanisms in both heterojunctions and MOSFET's, we also made measurements in Si/SiO_2 to provide an independent check on the accuracy of models which predict the relative ratio of the SdH and classical scattering times.

II. SCATTERING LIFETIMES

A. Classical lifetime measurements

When the simplified Boltzmann equation is solved in the relaxation-time approximation, the mean time between collisions is weighted by a factor of $1-\cos\theta$ as in the equation

$$1/\tau=\int dk' W_{k,k'}(1-\cos\theta)\ , \tag{1}$$

where $W_{k,k'}$ is the probability of scattering from state k to k' and θ is the scattering angle.

The relaxation-time approximation favors large-angle scattering over small-angle scattering due to the weighting factor of $(1-\cos\theta)$ in Eq. (1). Thus, if the relaxation-time approximation is assumed in systems where small-angle scattering dominates, the transport scattering time represents only a fraction of the actual number of collisions.

To allow a discussion of the various transport measurements in this paper, we will designate as the classical scattering time τ_c a scattering time derived from transport expressions assuming the relaxation-time approximation. The Drude mobility is related directly to the scattering time by

$$\mu=e\tau/m^*\ , \tag{2}$$

where m^* is the reduced mass. For measures of collision rates, the mobility and scattering time, as related by Eq. (2), will be used interchangeably.

Various methods (e.g., geometric magnetoresistance and magnetotransconductance) exist to obtain the classical scattering time τ_c from transport in a magnetic field. Complications exist when applying these techniques to TEGFET's because the current can flow in either the TEG or the parallel AlGaAs layer. In addition, stray effects such as parasitic resistance from ungated portions of the device channel and contact resistance can alter the apparent scattering time, making it difficult to single out the TEG layer. In a separate paper we will discuss the magnetoresistance and magnetotransconductance methods of obtaining the TEG scattering time. Here, we concentrate on measurements of the classical scattering time from the Hall technique,[9] with a four-point geometry and a gated van der Pauw pattern used to obtain the classical scattering time from the measured mobility via Eq. (2). The method is relatively insensitive to parasitic resistances since it is a four-point voltage measurement. Distortion of the TEG mobility stemming from lower-mobility electrons in the parallel AlGaAs layer are small even at zero gate voltage where the charge density in the AlGaAs is largest. The peak Hall mobility occurs at a value of gate bias where the AlGaAs is depleted so it measures the TEG only, and is suitable for determination of τ_c.

B. Quantum lifetime measurements

The SdH oscillatory conductivity reflects the shape of the collision-broadened Landau levels. The envelope of the oscillations is determined by the Landau-level linewidth and can be fitted to an expression[10] of the oscillatory magnetoconductivity. The collision broadening of the Landau levels is related to the collision scattering time by

$$\Gamma\tau=\hbar/2\ .$$

The magnetoconductivity in the Ando theory is, neglecting higher harmonics, to first order,

$$\sigma_{xx}=\left[\frac{\sigma_{xx}(B=0)}{1+(\omega_c\tau_q)^2}+\sigma_{\rm osc}\cos\left[\frac{2\pi E_f}{\hbar\omega_c}+\phi\right]\right]\ . \tag{3}$$

The conductance is the sum of the classical Drude conductivity plus an oscillatory term. The amplitude of the oscillatory conductivity $\sigma_{\rm osc}$ is,

$$\sigma_{\rm osc}=\frac{\sigma_{xx}(B=0)}{1+(\omega_c\tau_q)^2}K(B,T)A(B,\tau_q)e^{-\pi/\omega_c\tau_q}\ . \tag{4}$$

The oscillatory term is the product of a term $K(B,T)$ which describes the temperature broadening of the Fermi level,

$$K(B,T)=\frac{2\pi^2k_BT}{\hbar\omega_c}\,\mathrm{csch}(2\pi^2k_BT/\hbar\omega_c)\ ,$$

the usual exponential scattering factor, $\exp(-\pi/\omega_c\tau_q)$, in Eq. (4), and a pre-exponential term,

$$A(B,\tau_q)=\frac{2\pi(\omega_c\tau_q)^2}{1+(\omega_c\tau_q)^2}\ .$$

The scattering-time parameter τ_q is the measure of the broadening of the Landau levels from collisions. Because of the phase sensitivity of the wave function, the SdH sig-

nal is affected by even small perturbations and contributes to the several orders of magnitude difference between τ_q and τ_c in metals.[11] The scattering-time parameter in the SdH expression effectively measures the *entire* collision cross section; small- and large-angle scattering events are counted equally in dephasing the cyclotron orbits. Because the SdH scattering-time parameter is fundamentally different from that derived from classical transport measurements (e.g., Hall effect), the SdH scattering time will be referred to as the "quantum scattering time" τ_q.

There is a limit to the above argument; an arbitrarily small deviation of the electron momentum will not dephase the cyclotron orbit. The smallest angle which will cause dephasing is of order[11]

$$\theta_c = \pi/2\nu \,, \tag{5}$$

where ν is the Landau-level index. Since ν (for a given B) increases as N increases, θ_c is expected to decrease inversely as the TEG density increases. This result was derived simply from geometrical consideration of the increase in phase of an electron in a cyclotron orbit which is scattered through some angle θ. In a SdH measurement an electron scattered through an angle larger than θ_c will be removed from the measured oscillatory current. In AlGaAs/GaAs heterojunctions with typical TEG densities of 0.5×10^{12} cm^{-2}, the critical angle calculated using Eq. (5) is 10°.

An example of the oscillatory SdH data, obtained from measuring channel current as a function of the inverse magnetic field, is shown in Fig. 2. The envelope of the oscillations is extracted by Fourier-filtering[12] the data to remove the dc and slowly-varying terms, and then back-transforming the filtered data. Although measurements of the magnetotransconductance ($g_m \propto d\sigma/dV_g$) provide amplification of the SdH oscillatory structure, additional complications arising from terms proportional to $d\mu/dV_g$ make this method undesirable. The Fourier-filtering of the magnetoconductance provides a comparable enhancement of the oscillatory component without this complication.

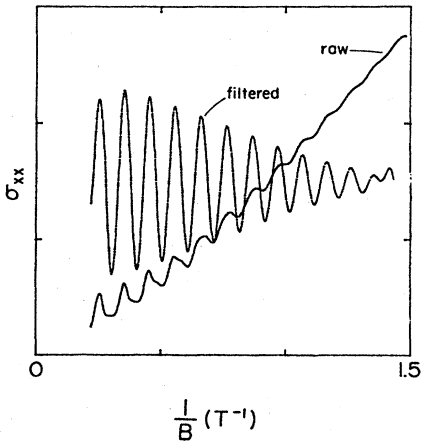

FIG. 2. SdH oscillations as a function of inverse magnetic field. The raw data show large, interfering low-frequency components as well as higher harmonic content, which are removed using the Fourier-filtering process. The data after filtering are shown superimposed over the original data.

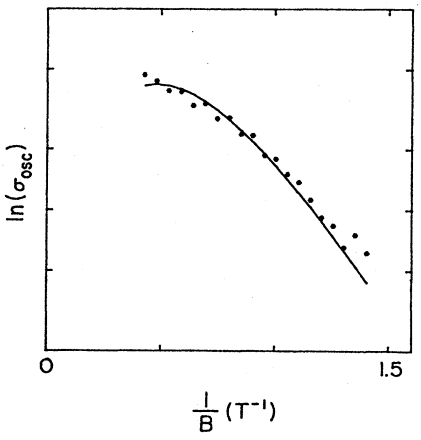

FIG. 3. Typical least-squares fit (solid line) using Eq. (4) with τ_q as an adjustable parameter to the SdH oscillatory envelope (discrete points) as a function of the inverse magnetic field.

The TEG scattering time, and hence mobility, may be obtained as a parameter in a least-squares fit of the amplitude envelope of the filtered data to Eq. (4). Figure 3 shows an example of the fitted data. The low-field straight line is bent over at high fields due to the pre-exponential factors in Eq. (4). This analysis is repeated at a series of voltages to obtain curves of τ_q versus V_g.

III. CALCULATED SCATTERING MECHANISMS

Dominant scattering mechanisms limiting TEGFET mobility have been the subject of lively interest. However, all such previous calculations have dealt with τ_c in order to understand mobility limits. No previous calculation addresses quantitative mechanisms for τ_q. In view of the fact that earlier experiments[11] in metals showed several orders of magnitude greater sensitivity to small-angle scattering for τ_q than for τ_c, an extension to TEG semiconductor systems seemed desirable.

The types of scattering which will be considered are ionized-impurity, interface-roughness, and alloy-disorder scattering. The classical scattering time is compared with a quantum scattering time which measures the total collision cross section to yield a quantum-to-classical scattering time ratio. The ratio is sensitive to the scattering mechanism used to calculate the cross section. This is the first systematic evaluation of the scattering-time—ratio technique to select between competing scattering mechanisms in TEG systems. This present calculation follows earlier work of Ando[3] and the symbol notation used is the same.

A. Impurity scattering

Under the broad classification of screened-Coulomb scattering, collisions with ionized-impurity charge centers are further divided into three subgroups depending on whether the impurity is located in the TEG, undoped AlGaAs buffer layer, or in the doped AlGaAs layer (Fig. 1). Most theoretical scattering models focus on centers out-

side the TEG layer, since the MBE GaAs layer is not intentionally doped, whereas the AlGaAs layer is heavily doped. Various theoretical expressions have been developed for the form of the scattering time from ionized impurities.[6,7] Ando has developed an expression for the classical scattering time which extends to AlGaAs/GaAs heterojunctions[3] earlier work done explicitly for Si MOSFET's,

$$\frac{\hbar}{\tau(k)}=2\pi\int_{-\infty}^{\infty}dz\,N_i(z)\sum_q\left[\left[\frac{2\pi e^2}{q\xi(q)}\right]^2|F_i(q,z)|^2\times(1-\cos\theta)\delta(\epsilon_k-\epsilon_{k-q})\right]. \tag{6}$$

The sum in this equation evaluates to

$$\sum_q[\ ]=\frac{m}{(2\pi\hbar)^2}\int_0^{2\pi}\left[\frac{2\pi e^2}{q\xi(q)}\right]^2|F_i(q,z)|^2(1-\cos\theta)d\theta\ . \tag{7}$$

The complexity of Eq. (6) makes it desirable to illustrate the calculation of the quantum-to-classical scattering-time ratio using the comparatively simple *unscreened* form of the differential cross section in two dimensions:[6]

$$\sigma(\theta)=\frac{G\tanh(\pi/G)}{2k\sin^2(\theta/2)}\ , \tag{8}$$

where

$$G=\frac{mZe^2}{k\bar{\kappa}\hbar^2}\ .$$

The scattering time is related to Eq. (8) via the integral

$$\frac{1}{\tau}=\int_0^{2\pi}\sigma(\theta)(1-\cos\theta)d\theta\ . \tag{9}$$

Evaluating the integral in the Eq. (9) using the unscreened differential scattering cross section of Eq. (8) gives

$$\frac{1}{\tau}=\frac{\pi G\tanh(\pi G)}{2k}\ . \tag{10}$$

However, as discussed in the preceding section, the factor of $1-\cos\theta$ should not be included in the integral of the cross section for the SdH quantum scattering time. In fact, omitting the factor of $1-\cos\theta$ is equivalent to counting *every* scattering event equally, and for unscreened-Coulomb scattering, leads to an infinite cross section, or equivalently, $\tau=0$. The SdH quantum scattering time at a given magnetic field is not affected by scattering events below a critical scattering angle θ_c, which sets the lower limit of integration. The quantum scattering time is related to the differential scattering cross section by

$$\frac{1}{\tau_q}=2\int_{\theta_c}^{\pi}\sigma(\theta)d\theta\ . \tag{11}$$

This integral may be evaluated exactly for unscreened-Coulomb scattering as

$$\frac{1}{\tau_q}=\frac{4G\tanh(\pi G)\cot(\theta_c/2)}{2k}\ .$$

Thus, the calculated quantum and classical scattering times predict the ratio of the measured SdH and classical (Hall effect, GMR) scattering times. For the present example with a 10° critical angle (Sec. II), the expected ratio of τ_q/τ_c is

$$\frac{\tau_q}{\tau_c}=\frac{\pi}{4}\tan(\theta_c/2)=0.07\quad(\theta_c=10^\circ)\ .$$

Figure 4 illustrates the dependence of this scattering time ratio as a function of the SdH critical angle θ_c. The ratio can differ greatly from 1. The scattering-time ratio falls to zero as θ_c approaches zero, where small-angle scattering is increasingly important.

This calculation can be extended for screened-Coulomb scattering using Eqs. (6) and (7), following the steps outlined above for the unscreened case. The integrands are more complicated, and rather than seeking a general solution, an explicit solution of the collision scattering time is found by numerical integration. The ratio of the scattering times as a function of the critical angle is shown for screened-Coulomb scattering in Fig. 5. Note that the TEG density used in evaluating Eq. (6) was $N=0.3\times10^{12}$ cm^{-2}, which was a typical zero-bias value of the electron density in the measured samples. The ionized Si donors were assumed to be separated from the TEG by the measured 80-Å undoped spacer layer. These values were also used in the evaluation of the interface-roughness expression that follows. At a critical angle of 10°, the quantum-to-classical scattering-time ratio is 0.14, a factor of 2 larger than the equivalent unscreened value. This reflects the fact that in the limit of small scattering angles the *screened* differential cross section is finite.

B. Interface-roughness scattering

A second plausible form of scattering arises from perturbations in the potential caused by "roughness" at the AlGaAs/GaAs interface. Scattering in the TEG by interface roughness has been studied in Si MOSFET systems; this type of scattering dominates there at high carrier densities.[8] Recently, calculations have been made for heterojunction devices that build upon the previous work done for Si MOSFET's.[3] The expression for the interface-roughness scattering time is

$$\frac{\hbar}{\tau(k)}=2\pi\sum_q\pi\left[\frac{\Delta dF_{\text{eff}}}{\xi(q)}\right]^2e^{-(qd/2)^2}(1-\cos\theta)\delta(\epsilon_k-\epsilon_{k-q})\ .$$

This result can be rewritten in integral form as

$$\frac{\hbar}{\tau(k)}=2\pi\frac{m}{(2\pi\hbar)^2}\int_0^{2\pi}\pi\left[\frac{\Delta dF_{\text{eff}}}{\xi(q)}\right]^2e^{-(qd/2)^2}(1-\cos\theta)d\theta\ . \tag{12}$$

The scattering-time—ratio values as a function of the critical angle are shown for interface-roughness scattering in Fig. 6. We choose $\Delta=4$ Å, $d=15$ Å as in Ando.[3] Note

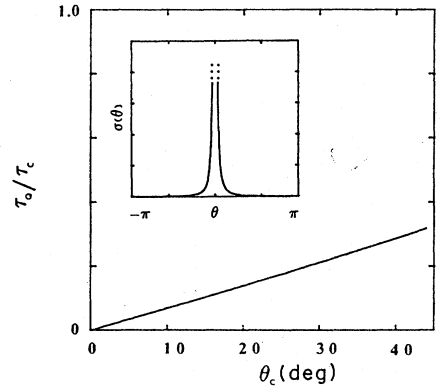

FIG. 4. The ratio of the quantum and classical scattering times, τ_q/τ_c, for an unscreened-Coulomb potential as a function for the SdH critical scattering angle θ_c. The scattering-time ratio is small (compared to 1) over a wide range of θ_c. The inset shows the corresponding form of the differential scattering cross section. The value of $\sigma(\theta)$ is singular at $\theta=0°$, reflecting the long-range nature of the Coulomb potential.

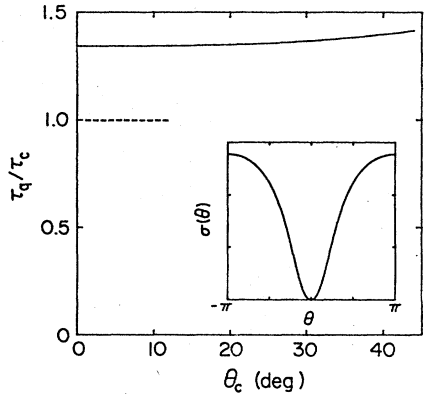

FIG. 6. The scattering-time ratio τ_q/τ_c for interface-roughness scattering. The inset shows the corresponding differential cross section. Note that the values are larger than 1, in contrast to Fig. 5.

from the results in Fig. 6 that there is a significant *qualitative* difference between the calculated scattering-time ratio assuming interface-roughness scattering compared to the screened-Coulomb case. While the precise form does depend on the choice of Δ and d, it is a general feature that interface-roughness scattering is predominantly large angle. The calculated ratio τ_q/τ_c is nearly 1 for interface scattering; this agrees remarkably well with earlier experiments which indicated equality between the classical and quantum scattering times in Si MOSFET's.[5]

Obviously, direct measurement of the quantum-to-classical scattering-time ratio is necessary to resolve whether interface-roughness scattering is dominant. However, evidence suggests that the atomically abrupt heterojunction interface is smooth.[13] This is expected because in AlGaAs/GaAs MBE heterojunctions the overlying AlGaAs lattice is matched to the GaAs one to within a few tenths of a percent. In contrast, the SiO_2 dielectric used in Si MOSFET's is (a) not well lattice-matched to the underlying Si, (b) polycrystalline, and (c) adsorbed into the Si layer. Therefore, interface-roughness scattering is not expected to play the dominant role in electron scattering in AlGaAs/GaAs heterojunctions that it plays in Si MOSFET's.

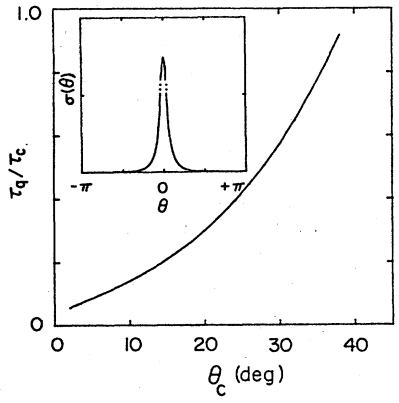

FIG. 5. The scattering-time ratio τ_q/τ_c for a *screened*-Coulomb potential as a function of critical scattering angle θ_c. The inset shows the differential scattering cross section. In contrast to the unscreened case, τ_q/τ_c is finite at $\theta_c=0°$ due to the screening. The scattering-time ratio increases faster than in the unscreened case, but only approaches unity for very large values of θ_c ($\approx 40°$).

C. Alloy-disorder scattering

During the growth of the heterojunction devices an undoped AlGaAs buffer layer of order 100 Å is intentionally placed between the Si-doped AlGaAs layer and the underlying GaAs layer to spatially isolate the ionized donors in the lower-mobility AlGaAs. In placing the buffer layer containing some fraction of Al directly against the GaAs, alloy-disorder scattering becomes a third possible contribution to the TEG scattering mechanisms. The theoretical limit for the mobility, $\mu \propto (\hbar/\tau)^{-1}$, from alloy-disorder scattering is of the order of 10^7 cm^2/V s. This is 2—3 orders of magnitude larger than comparable predictions[3] of other scattering mechanisms for heterojunction layers with comparable TEG densities. Since the mobility of the heterojunctions used in this work have mobilities closer to 10^4 and 10^5 cm^2/V s, we may safely assume that alloy-disorder scattering is not a dominant contribution to the scattering time in our samples.

To summarize, three principle forms of scattering have been examined: ionized charge center, interface roughness, and alloy disorder. Alloy-disorder scattering is not expected to play a large role in AlGaAs/GaAs heterojunctions and it is rejected as a dominant mechanism since the predicted mobility limit is up to 3 orders of magnitude larger than the measured mobility in the devices studied. Interface roughness is also not anticipated to play a large role in the scattering time since the heterojunction interface is atomically smooth. The form of interface-roughness scattering is such that the quantum-to-classical scattering-time ratio is close to 1.0. Such a clear signature of this type of scattering is experimentally easy to dif-

ferentiate from screened-Coulomb scattering, which yields scattering-time ratios differing by an order of magnitude or more depending on the TEG density. On the basis of the above considerations, it is predicted that screened Coulomb is the dominant form of scattering in the TEG at the AlGaAs/GaAs heterojunction interface.

IV. RESULTS

The discussion of the results obtained from this work will be divided into three parts. The first part deals with the classical mobility measurements. The second part is a discussion of the quantum scattering times as measured by the SdH oscillation envelope. The third part presents the quantum-to-classical scattering-time ratio and discusses the fit to the various predicted ratios from the preceding section.

A. Classical lifetimes

The Hall mobility was measured over a temperature range of 300 to 1.3 K. A substantial increase in mobility was observed between the 300- and the 1.3-K measurements. A decrease in the channel pinch-off voltage of approximately 500 mV was noted between 300 and 1.3 K, due to the charge-depletion regions in the AlGaAs expanding as the donor charge density partially freezes out at the lower temperatures. The peak value of the Hall mobility for the low-mobility wafer is 40 000 $cm^2/V\,s$ at 1.3 K and 6200 $cm^2/V\,s$ at 300 K, corresponding to scattering times of 1.5 and 0.2 ps, respectively. For the high-mobility wafer the peak mobility, 117 000 $cm^2/V\,s$, corresponds to a scattering time of 4.5 ps, a factor of 3.0 larger than that of the low-mobility wafer.

B. Quantum lifetimes

The quantum scattering time was measured on both the high-mobility and the low-mobility wafers using a series of different short-gate devices. The measurements were made a temperature of 1.3 K while the samples were in complete darkness. The issue of ambient light was a concern because of the persistent photoconductivity effect,[14] which can increase the TEG density in a manner which is difficult to control. At discrete values of the gate voltage, the magnetic field is swept and the resulting oscillating conductivity waveform is used to obtain a single scattering-time value. The scattering time is obtained from a single-parameter least-squares fit to the Ando expression [Eq. (4)]. The measured parameters in Eq. (4) were the magnetic field B, the temperature T, and the $B=0$ value of the conductivity, $\sigma(0)$. As a check of the fitting method, $\sigma(0)$ was left as a variable during the fit of τ_q. The best-fit values of $\sigma(0)$ were typically within 10—30% of the measured values. This is remarkable agreement since $\sigma(0)$ is a prefactor to the exponential term containing τ_q and has little effect on the overall *shape* of the oscillations. The agreement between the fitted and measured $\sigma(0)$ confirms that the *absolute* amplitude of the oscillations is correctly predicted by Eq. (4).

Figure 7 shows the SdH quantum scattering times obtained from both wafers. The quantum scattering time is

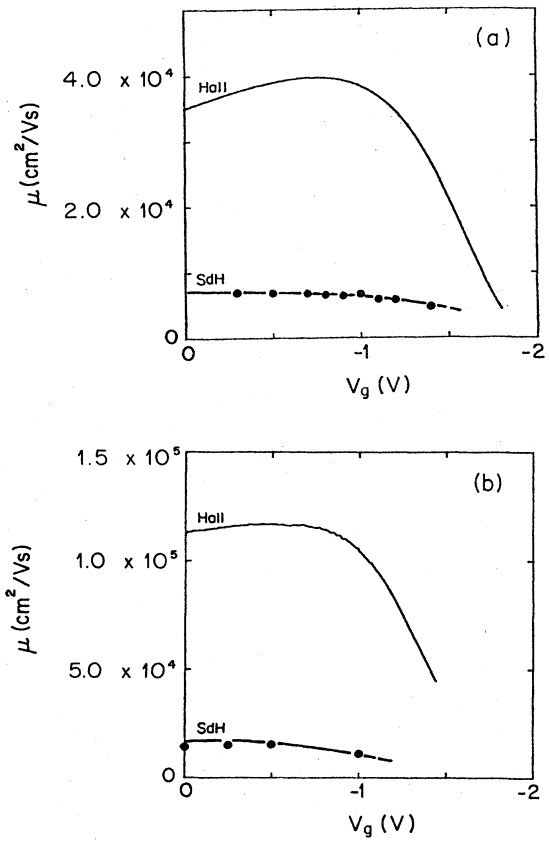

FIG. 7. Comparison of classical (Hall) and quantum (SdH) mobilities. (a) Data are from the low-mobility wafer. (b) Data are from the high-mobility wafer.

insensitive to the gate bias from −0.25 to −1.5 V because the TEG density remains constant there. As the gate voltage approaches pinch-off, the quantum scattering time shows a monotonic decrease seen in the classical scattering times. The same qualitative features are found in both the low-mobility and the high-mobility wafers although the quantum scattering time values differ by a factor of 2. For the lower-mobility wafer, it was difficult to obtain quantum scattering times near pinch-off because the decreasing TEG density produced fewer oscillations during a sweep of the magnetic field, making the envelope analysis difficult and prone to error.

C. Quantum-to-classical lifetime ratio

A dramatic feature is immediately apparent (Fig. 7) upon comparing the quantum and classical scattering-time measurements. The classical scattering times are obtained from classical mobilities discussed above, via Eq. (2). The quantum scattering time is smaller than the classical scattering time by an order of magnitude. Table I lists the values of the peak classical scattering times and the quantum scattering time for both the low- and high-mobility wafers. The lower-mobility wafer was lower quantum and classical scattering times by a factor of 2—3

TABLE I. Classical (Hall) and quantum (SdH) mobilities and corresponding lifetimes for both MBE wafers.

	Mobility ($cm^2/V\,s$)	
	Hall	SdH
Low-mobility wafer	40 000 (1.5 ps)	7000 (0.3 ps)
High-mobility wafer	117 000 (4.5 ps)	14 140 (0.5 ps)

compared to the high-mobility wafer. Figure 7(a) shows the scattering times τ_c and τ_q for the low-mobility wafer plotted together for comparison as a function of gate bias. Figure 7(b) is the corresponding plot for the high-mobility wafer. Given the theory of the quantum-to-classical scattering-time ratio introduced in Secs. II and III, these data allow a determination of the limiting scattering mechanism at the TEG heterojunction interface. The scattering-time ratio τ_q/τ_c, as a function of gate bias, is plotted in Fig. 8 for both wafers. The classical scattering time used here is from the Hall measurements. The scattering-time ratio is nearly constant away from the pinch-off gate bias. The scattering time ratio for the high mobility wafer is consistently lower than the ratio for the other wafer.

The same quantum-to-classical scattering-time measurements have been made in a Si/SiO_2 MOSFET. The data for both the quantum and classical scattering times (here in terms of the mobility $\mu=e\tau/m$) as a function of gate bias are presented in Fig. 9. As the calculations developed in Sec. III predict, the classical scattering time is closely correlated with the quantum scattering time measured via SdH. These MOSFET quantum and classical scattering-time measurements agree with earlier studies made on similar systems,[5] and establish the validity of our data analysis (both the Fourier filtering and the fits to the Ando theory).

Figure 10 is the graph of the scattering-time ratio τ_q/τ_c as a function of the critical scattering angle for the high- and low-mobility wafers. The calculated ratio from screened and unscreened impurity scattering and a competing mechanism (interface-roughness scattering) are overlayered on the graph for comparison with data. Included in this figure is the MOSFET τ_q/τ_c ratio for comparison with the interface-roughness curve and for contrast with the MBE heterojunction results. The data for the high-mobility wafer are in excellent agreement with the predicted ratio given by the impurity scattering curve

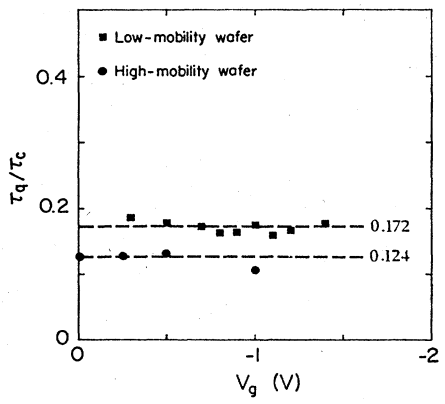

FIG. 8. The quantum-to-classical scattering-time ratio τ_q/τ_c for the high-mobility and low-mobility wafers as a function of gate bias.

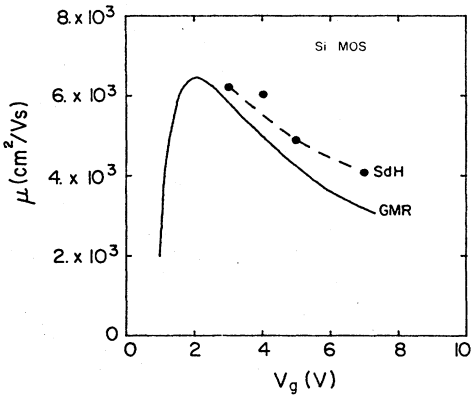

FIG. 9. The GMR and SdH quantum scattering times (plotted in terms of the equivalent mobility) as functions of gate bias for a Si MOSFET, measured in our laboratory with analysis methods identical to those used for GaAs (Figs.7 and 8). The region to the right of the mobility peak decreases with increasing gate voltage (TEG density), in agreement with theoretical models assuming surface-roughness scattering (Ref. 8).

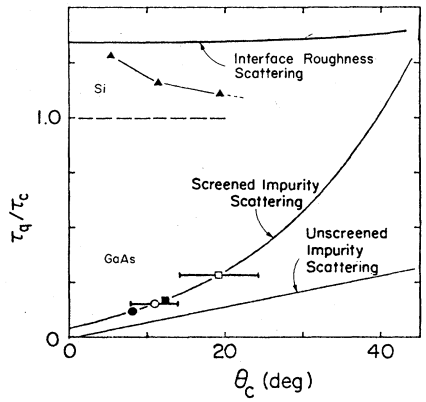

FIG. 10. Comparison of the measured τ_q/τ_c scattering-time ratio and the calculated ratios (solid curves), from Sec. III, as a function of the SdH critical scattering angle. Data from both the high-mobility (●) and low-mobility (■) MBE heterojunction wafers are shown. Also included is the Si MOSFET scattering-time ratio (▲). The theoretical ratios (open symbols) are deduced from the intersection of the impurity scattering curve and the calculated critical scattering angle [obtained from Eq. (5)] for both MBE wafers. The open square (□) is the calculated value for the low-mobility wafer and the open circle (○) is the corresponding value for the high-mobility wafer. The error bars for the theoretical ratios reflect the uncertainty in θ_c introduced by sweeping the magnetic field (i.e., the Landau index) to obtain the SdH quantum scattering time.

and the expected critical scattering angle. The ratio for the low-mobility wafer is somewhat smaller than expected, but is still in reasonable agreement. Qualitatively, the separation of the scattering-time ratios of the two wafers makes sense because the higher-mobility wafer has a larger TEG density, which correspondingly means higher Landau-level indices and a smaller critical scattering angle.

The values of the theory points are based on a calculation of θ_c which depends on the Landau index, i.e., the TEG density and the value of the magnetic field [Eq. (5)]. The TEG density, controlled by the gate voltage, remained fixed. Although the magnetic field value changed during a SdH data window, the resulting change in the critical angle only deviated by 4°—10° as a result of the changing field. The measured quantum-to-classical scattering-time ratio most closely agrees with the predicted ratio for values of θ_c corresponding to the *low*-magnetic-field portion of the SdH data.

In conclusion, these data strongly support the prediction of screened ionized-impurity scattering as the limiting scattering mechanism at low temperatures. These data support this conclusion in several ways. First, the data closely match the predicted scattering-time ratio, and even though the two wafers have quite different quality (the classical scattering time of the two wafers differs by a factor of 3.0) both the quantum-to-classical scattering-time ratios fit the theoretical result for ionized-impurity scattering. If the higher-mobility wafer were sufficiently pure to sense the next weakest scattering mechanism (e.g., interface roughness or alloy disorder), then the scattering-time ratio result would not fit the same scattering curve (Fig. 10) as the lower-mobility wafer. Thus, these results demonstrate that both samples are solidly in the regime dominated by ionized-impurity scattering. This agrees very well with recent calculations of the mobility for the various contributions to the scattering in the TEG. Table II lists the predicted[3] classical mobilities from various scattering mechanisms. On the basis of the predictions and these data, it is expected that a low-temperature mobility of at least 10^6 cm^2/V s would be necessary to observe the next weakest scattering regime via the quantum-to-classical scattering-time ratio.

TABLE II. Theoretical predictions (Ref. 3) of the AlGaAs heterojunction mobility with the scattering mechanism as a parameter. The range of the values shown corresponds to the measured TEG densities of the two MBE wafers. The first value matches the TEG density for the low-mobility wafer.

Scattering mechanism	Mobility (cm^2/V s)
Ionized-impurity scattering	$(1.1-1.6)\times10^5$ ($N_D-N_A=2\times10^{17}$ cm^{-3}) ($N_{\text{depl}}=5\times10^{10}$ cm^{-2})
Surface-roughness scattering	$(3.0-1.2)\times10^6$
Alloy-disorder scattering	$(5.0-2.0)\times10^6$ ($N_{\text{depl}}=1.0\times10^{10}$, $x=0.2$)

The successful prediction of the τ_q/τ_c ratio in a MOSFET system, where the TEG mobility is limited by interface-roughness scattering, is evidence that the scattering in the MBE TEG is limited by a different mechanism (i.e., ionized-impurity scattering). In the MOSFET TEG the predicted quantum scattering time is actually *larger* than the corresponding classical scattering time; there is thus a qualitative difference between the predictions of scattering mechanisms. The measured MOSFET scattering times agree with the predicted scattering-time ratio, lending confidence to both the measurement technique and the theoretical method developed in the preceding two sections.

V. SUMMARY

The transport scattering times τ_q and τ_c have been measured in AlGaAs/GaAs heterojunction devices by classical (Hall) and quantum (SdH) techniques. The classical transport scattering time is accurate only for those materials where the angular distribution of the scattering is not predominantly of small-angle type. At higher magnetic fields, the Landau-level broadening is an effective measure of *every* scattering event above a small-angle limit θ_c.

A method of calculating the ratio of τ_q/τ_c has been developed. The classical scattering time τ_c is calculated from the integral of the differential cross section in the usual fashion with the inclusion of the $1-\cos\theta$ weighting factor. The SdH quantum scattering time τ_q is obtained by modifying the limits of the scattering integral to ignore collisions below θ_c and count every collision with $\theta>\theta_c$ by exclusion of the $1-\cos\theta$ weighting. The ratio of τ_q/τ_c calculated in this way is sensitive to the angular distribution of the differential cross section, which, in turn, depends on the particular model of scattering considered.

Three likely scattering mechanisms have been examined: alloy-disorder, interface-roughness, and screened-Coulomb scattering from ionized charge centers in the AlGaAs. The scattering-time ratio τ_q/τ_c for ionized-impurity scattering (0.14 at $\theta_c=10°$) is small compared to τ_q/τ_c for interface-roughness scattering. The qualitative difference between τ_q/τ_c for ionized-impurity scattering and competing scattering mechanisms allows a confident choice of the dominant mechanism from measured quantum and classical scattering times.

Results from two MBE wafers of very different quality have been presented. The low-mobility MBE wafer has a Hall mobility of 40 000 cm^2/V s or, equivalently, a scattering time of $\tau_c=1.5$ ps. The high-mobility wafer has a Hall mobility of 117 000 cm^2/V s, or $\tau_c=4.5$ ps.

The measured values of τ_q are nearly an order of magnitude smaller than τ_c. The averaged quantum-to-classical scattering-time ratios are 0.172 and 0.124 for the low-mobility and high-mobility wafers, respectively. Both these ratios are in very good agreement with the predicted scattering-time ratio from the screened ionized-impurity scattering calculation and confirm that it is the dominant mechanism. Although the high-mobility wafer might be expected to show influences of the next weakest scattering mechanism, this was not found to be the case. Despite a scattering time (either τ_c or τ_q) of ≈3.0 larger than the low-mobility wafer, the data from the high-mobility wafer

actually fit the impurity scattering model better. This is additional evidence that both MBE wafers are dominated by ionized-impurity scattering (a situation not expected to change until devices of mobilities of order 10^6 cm^2/V s are measured) and confirms existing theoretical calculations for the classical mobility in MBE AlGaAs/GaAs heterojunctions.[3] These results are additionally confirmed by the τ_c and τ_q data measured with a completely different system, the Si MOSFET. Our MOSFET results are in excellent agreement with the predicted scattering-time ratio for systems dominated by interface-roughness scattering. The ratio τ_q/τ_c is measured to be 1.1 at low gate bias, increasing to 1.3 at higher biases. These measurements confirm earlier theoretical models[8] and experimental measurements[5] of the TEG at the SiO_2/Si interface. In addition, our MOSFET results constitute experimental support for the validity of the method developed here for calculating the scattering-time ratio τ_q/τ_c from the form of the differential cross section. A systematic investigation of competing effects which might interfere with the accurate determination of the τ_q, presented in the Appendix, indicates that no known stray effect was large enough to be of concern in our samples.

ACKNOWLEDGMENTS

The portion of this research performed at the University of Oregon was sponsored by the National Science Foundation Division of Materials Research, under Grant No. DMR-81-19550, and by the Tektronix Foundation. This project was initiated when one of us (R.J.H.) was visiting Thomson CSF, and all device fabrication was carried out at that institution. We thank R. Wallis, J. Chevrier, D. Delagebeaudeauf, and D. Pons for helpful discussions, and R. Cordeau for technical assistance at Thomson CSF; we are grateful to R. Haydock and J. D. Cohen of the University of Oregon for several stimulating discussions.

APPENDIX: ANALYSIS OF COMPETING EFFECTS

This study represents the first quantitative analysis[1] of SdH data to obtain the quantum scattering time τ_q in a MBE heterojunction. In this appendix we investigate several potential interfering effects and demonstrate that they have no significant effect on the derived quantum scattering time.

1. Inhomogeneity broadening

The frequency of the SdH conductivity oscillations is a direct function of the TEG density:

$$\sigma \propto \cos\left[\frac{2\pi f}{B}\right], \quad f=\frac{\pi\hbar N}{e} .$$

If the TEG density is constant throughout the device channel, then the scattering time measured via the SdH technique corresponds to the true Landau-level width due to scattering. However, if portions of the TEG are at different densities, the overall amplitude of the SdH oscillations may be altered due to phase cancellation. Phase smearing alters the SdH envelope and reduces the measured quantum scattering time. The effect is to broaden the apparent Landau-level width; hence the term "inhomogeneity broadening."

The change in density necessary to phase-cancel the conductivity oscillations is

$$\Delta N = eB/2\pi\hbar .$$

Depending on the field value chosen, the value of ΔN required for phase cancellation varies between 8% and 32% of typical measured TEG densities.

Alternatively, one can estimate a value of ΔN which would result in the observed quantum-to-classical scattering-time ratio. The measured τ_q for the low-mobility layer corresponds to a mean Landau-level linewidth of 2.2 meV. The change in the TEG density which would account for the observed $\tau_c = 0.21$ meV is

$$\Delta N = m\Delta E_f/\pi\hbar^2 = 5.1\times10^{10}\ \text{cm}^{-2} .$$

This corresponds to a percentage change in the measured TEG density of 17%.

Such large TEG-density variations are *not* expected on our samples. Independent sheet-resistance measurements on the heterojunction wafers used in this work indicate an interpolated density variation of approximately 0.5% across the largest device dimensions.[15] This is almost an order of magnitude smaller than the value calculated to produce the observed quantum-to-classical scattering-time ratio.

Although the resistance measurements are a convincing measure of the large-scale density homogeneity (compared to a cyclotron orbit radius), they are not sensitive to microscopic inhomogeneities. Microscopic disorder, in the Si-dopant homogeneity, for example, might result in TEG-density variations. However, the MBE process is carried out at low temperatures ($\approx$600 °C) and lateral diffusion of the MBE constituents is unlikely. Variation in N could also come from variation in AlGaAs thickness; however, our AlGaAs layers were sufficiently thick that N is insensitive to variation in the etched thickness at the top of the AlGaAs.

Finally, the *measurements* of the quantum scattering time do not support a picture of phase cancellation resulting in alteration of the oscillation envelope. No evidence was seen of "beating" from phase cancellation of the conductivity oscillations or of low-field amplitude anomalies. In addition, variations between the values of the SdH TEG density between devices on the same wafer were small, typically less than 1%. The conclusion is that inhomogeneity broadening is not a significant influence on the measured quantum scattering time in our samples.[16]

2. Temperature effects

Temperature-broadening effects must also be considered since what is measured is effectively $(1/\tau_{\text{scatt}} + 1/\tau_T)^{-1}$. The temperature term depends on an accurate measurement of the lattice temperature and on thermal equilibrium between the TEG and the lattice. During the least-squares fit of the quantum scattering time, the temperature is normally set to the measured

sample temperature. When the temperature is left as a variable parameter (fixing the quantum scattering time equal to the large *classical* value), the least-squares fit of the TEG temperature is 9 K. The measured operating temperature is an order of magnitude smaller, typically 1.3 K, so errors in measuring the absolute temperature cannot account for the observed quantum-to-classical scattering-time ratio.

Hot-electron effects were also considered, but were eliminated as a source of error in the measured τ_q. The source-drain electric field was always smaller than 0.3 V/cm, which is below published[17] lower bounds for observing hot-electron effects in GaAs. As a check, measurements were made on the low-mobility wafer, indicating that an increase in the channel electric field by a factor of 10 above the typical field used for SdH measurements did not effect the quantum scattering time. This confirms that the TEG was in good thermal equilibrium with the measured lattice temperature.

3. Geometry effects

Distortion of the transverse conductivity from the small Hall electric field in a short-gate device was considered as a possible source of error for τ_q. Attempts have been made to correlate theory to experimental measurements of the channel current of rectangular device geometries in high magnetic fields.[18,19] According to the theory developed by Wick for an arbitrarily shaped two-dimensional sample in a magnetic field, the diagonal component of the conductivity is given as[18]

$$\sigma_{xx}=\frac{I_{sd}}{V_{sd}}\frac{1}{g(\sigma_{xx}/\sigma_{xy})},$$

where the function $g(\ )$ depends on the sample length-to-width (L/W) ratio and the size of the channel contacts. In moderate magnetic fields ($\omega_c\tau\approx 1$), $g(\ )$ is a small correction term to the channel current. Even for a relatively large L/W ratio is 1/3, the function $g(\ )$ is nearly constant and close to the Corbino geometry limit of W/L for the magnetic field ranges used in this work (less than 4.0 T).[19] The device geometries used for SdH measurements varied from $L/W=0.05$ (best case) to $L/W=0.29$ (worst case).

An empirical check was made on a series of short-gate TEGFET's with widely varying L/W ratios. The resultant quantum lifetimes showed no significant difference when compared for samples having L/W extremes of 0.05 and 0.29. We conclude from this empirical check, which is compatible with existing theory,[17,18] that a small Hall electric field in a short-gate TEGFET is not significant in explaining the observed difference between the quantum and classical scattering times.

[1]J. P. Harrang, R. J. Higgins, R. K. Goodall, P. R. Jay, M. Laviron, N. T. Linh, and R. H. Wallis, Bull. Am. Phys. Soc. **28**, 407 (1983); J. P. Harrang, R. J. Higgins, R. K. Goodall, P. R. Jay, M. Laviron, P. Delescluse, and R. H. Wallis, *ibid.* **29**, 472 (1984).

[2]S. Hiyamizu, J. Saito, K. Nanbu, and T. Ishikawa, Jpn. J. Appl. Phys. **22**, L609 (1983).

[3]T. Ando, J. Phys. Soc. Jpn. **51**, 3893 (1982).

[4]G. Bastard, Surf. Sci. **142**, 284 (1984); W. Walukiewicz, H. E. Ruda, J. Lagowski, and H. C. Gatos, Phys. Rev. B **30**, 4571 (1984); F. Stern, Appl. Phys. Lett. **43**, 974 (1983).

[5]F. F. Fang, A. B. Fowler, and A. Hartstein, Phys. Rev. B **16**, 4446 (1977).

[6]F. Stern and W. E. Howard, Phys. Rev. **163**, 816 (1967).

[7]T. Ando, A. B. Fowler, and F. Stern, Rev. Mod. Phys. **54**, 437 (1982).

[8]T. Ando, J. Phys. Soc. Jpn. **43**, 1616 (1977).

[9]L. J. van der Pauw, Philips Res. Rep. **13**, 1 (1958).

[10]T. Ando, J. Phys. Soc. Jpn. **37**, 1233 (1974).

[11]D. W. Terwilliger and R. J. Higgins, Phys. Rev. B **7**, 667 (1973); R. J. Higgins H. Alles, Y. K. Chang, and D. W. Terwilliger, in *Proceedings of the XIIIth International Conference on Low Temperature Physics, Boulder, 1972,* edited by K. D. Timmerhaus (Plenum, New York, 1974), p. 185. Equation (5) is readily derived following the original Onsager-Bohr-Sommerfeld approach, by calculating when the orbit area *added* by a small-angle scattering event contributes a 180° phase shift (see Fig. 2 of the latter reference).

[12]T. G. Matheson and R. J. Higgins, Phys. Rev. B **25**, 2633 (1982).

[13]H. Okamoto, M. Seki, and Y. Horikoshi, Jpn. J. Appl. Phys. **22**, L367 (1982).

[14]D. V. Lang, Phys. Rev. B **19**, 1015 (1979).

[15]Data supplied to R. J. Higgins by N. T. Linh (private communication).

[16]A recent publication [M. A. Paalanen, D. C. Tsui, and J. C. M. Hwang, Phys. Rev. Lett. **51**, 2226 (1983)] appearing after this work was completed (Ref. 1 above) touches on the issue of inhomogeneous broadening contributions to the measured scattering time. While these authors estimate that inhomogeneous broadening is a dominant contribution, our checks (see Appendix) indicate a negligible contribution in our samples. The difference is quite simply explained by differences in mobility (theirs were higher) and homogeneity (ours is presumably higher) which place our measurements squarely in the regime where impurity scattering can be studied without inhomogeneous broadening complications.

[17]J. Shah, A. Pinczuk, H. L. Stormer, A. C. Gossard, and W. Wiegmann, Bull. Am. Phys. Soc. **28**, 448 (1983).

[18]R. F. Wick, J. Appl. Phys. **25**, 741 (1954).

[19]S. Kawaji, Surf. Sci. **73**, 46 (1978).